Paper No. # 92

# Life Cycle Cost Analysis of Low Ductility RC Frame Buildings Retrofitted by Modern Retrofit Techniques

**Fabio FREDDI 1***
Polytechnic University of Marche, Department of Construction, Civil Engineering and Architecture
Via Brecce Bianche, 60131, Ancona, Italy
f.freddi@univpm.it,

**Jamie Ellen PADGETT 2**
Rice University, Department of Civil and Environmental Engineering
6100 Main Street, MS 318, Houston, TX 77005, USA
jamie.padgett@rice.edu,

**Andrea DALL'ASTA 3**
University of Camerino, Department of Architecture and Design
Viale Rimembranza, 63100 Ascoli Piceno, Italy
andrea.dallasta@unicam.it

## ABSTRACT

Many reinforced concrete (RC) frame buildings designed before the introduction of modern seismic codes are highly vulnerable to seismic actions due to their reduced ductility capacity. Passive control systems have emerged to be efficient tools for the seismic retrofit of low ductility RC frames and help to reduce economical losses in consequence of seismic events. Since funds to investment for seismic vulnerability reduction may be limited, a risk-based life cycle cost analysis approach is required to evaluate and compare the cost effectiveness of different mitigation strategies. In this paper, several retrofit methods are compared. In particular, superelastic Shape Memory Alloys braces or Buckling Restrained Braces are investigated for their effectiveness in reducing seismic vulnerability and losses. A benchmark two-dimensional reinforced concrete frame with low ductility capacity is considered as a case study. The frame is designed for gravity-load only and does not comply with modern seismic code requirements. The retrofit devices are designed in a way to obtain the same base shear capacity for the two retrofitted frames. The study to evaluate the effectiveness of the retrofit is conducted by a probabilistic approach where the seismic record-to-record variability is modeled by using a suite of recorded ground motions, and nonlinear time history analyses are performed to generate samples of the demand. Fragility curves are generated for slight, moderate, extensive and collapse limit states. Finally, the comparison among the different retrofit methods is conducted by performing a Seismic Life Cycle Cost Analysis and by evaluating the loss saving for each method.

**Keywords:** *Vulnerability of reinforced concrete frames, seismic retrofit, fragility, life-cycle cost.*

## 1 INTRODUCTION

The damage occurred during recent earthquakes in many existing reinforced concrete (RC) buildings designed before the introduction of modern seismic codes has shown that these structures are very vulnerable to seismic action due to their reduced ductility capacity. Thus, there is a significant need of modern and effective retrofit techniques for increasing their safety and reducing



* Corresponding author

social and economical losses in consequence of seismic events. Among the various techniques currently employed for the retrofit, the use of dissipative braces appears to be very promising [1]. These braces provide a supplemental load path for the earthquake induced horizontal actions and thus enhance the seismic behaviour of the frame by adding dissipation capacity and, in some cases, stiffness to the bare frame depending on the device used within the brace. In this paper, the adoption of different devices, such as superelastic Shape Memory Alloys (SMAs) and Buckling Restrained Braces (BRBs) is investigated.

Since resources for seismic retrofit are often limited and uncertainty exists in the performance of the as-built and retrofitted systems, a risk-based life cycle cost (LCC) analysis offers an ideal approach to evaluate and compare the effectiveness of different mitigation strategies. The LCC of a structure includes the costs that the owner incurs along the structure's life time ranging from initial construction, maintenance and repair, to deconstruction costs. In particular, the contribution of repair cost as consequence of extreme events has been emphasized by many studies along the last years [2][3], and often applied in consideration of losses attributed to seismic damage. The LCC analysis has been used in Wen and Shinozuka 2001 [4] evaluating the cost-effectiveness of active structural control systems. In past studies [5], building design criteria are developed by minimizing the expected total LCC with respect to the design loads and resistance. In others [6], a methodology based on seismic LCC and cost-benefit ratio (CBR) is proposed and applied in order to evaluate the best retrofits techniques for bridges. Moreover, innovative seismic codes [7], standardize the LCC evaluation for different structural typologies, including the social and economical losses.

In this paper, a RC low-ductility frame is retrofitted by using dissipative braces made by placing in series an elastic steel brace and a dissipative device. The case study chosen for the application is a three story ordinary RC moment resisting frame designed for gravity loads only and without any seismic detailing and it is representative of low-rise buildings constructed in the Eastern and Central United States. The frame was largely experimentally investigated by Bracci et al. 1992 [8] and the experimental results are available in literature allowing an accurate validation of the finite element (FE) model.

The seismic LCC analysis implies evaluation of seismic risk that is performed by using a probabilistic approach. In this paper, the interstory drift (IDR) and the story acceleration are used as engineering demand parameters (EDPs) in order to evaluate the structural, non-structural and contents damage as suggested in HAZUS-MH 2.0 [7] and fragility curves are developed in a closed form as by following the methodology proposed in Cornell et al. 2002 [9]. Four different limit states (LSs) are considered (Slight, Moderate, Extensive and Collapse) and the corresponding repair costs are defined as in HAZUS-MH 2.0 [7]. Finally, the comparison among the different retrofit methods is conducted by performing a seismic LCC analysis.

## 2 METHODOLOGY

Evaluation of costs associated with seismic events, considered as the only type of extreme event in this paper requires integration of information regarding the seismic hazard, structure performance and cost associated with the building damage. The LCC analysis for seismic retrofit effectiveness evaluation emphasizes the potential costs due to seismic damage and does not address building maintenance cost within the scope of this study and hence the only seismic losses (SLs) are considered. The SLs modeling framework is presented in this section and will be applied in the following sections for the building retrofit evaluation. Seismic ground motion (g.m.) intensity is usually described by a seismic hazard curve $H(im)$ which provides the annual probability of exceeding specified levels of intensity measure (IM). Nonlinear time history analyses (NTHAs) are performed by using a set of g.m. records which allows to represent g.m. variability in terms of frequency contents, duration and amplitude pushing the structure in all the range from the elastic behavior, inelastic behavior up to collapse. Then, Probabilistic Seismic Demand Models (PSDMs) are defined in order to synthetically describe the structural response. They provide the relationships between the demand on a structural Engineering Demand Parameters (EDPs) and the ground motion shaking intensity. The demand on the component $k$ is synthesized by describing the relation between the median structural demand $\widehat{D}_k$ and the IM by power model as suggested in Cornell et al. 2002 [9]. In order to complete the probabilistic representation, the demand is traditionally assumed as lognormally distributed with logarithmic standard deviation $\beta_{D,k}$. Homoschedasticity of the demand ($\beta_{D|IM,k}=\beta_{D,k}$) is assumed. Fragility curves quantify the vulnerability of the system with respect to a specified level of damage, termed as damage state (DS). The seismic fragility curves are defined in a closed form by using the PSDMs as suggested in Cornell et al. 2002 [9]. The probability that a certain value of the demand ($D_k$) exceeds the capacity ($C_{k,i}$) defined by the $i^{th}$ damage state ($DS_i$) is written as follow:

$$P\left[DS_{k,i}\left|IM=im\right.\right]=1-\Phi\left[\frac{\ln\left(\widehat{C}_k\left|DS_i\right.\right)-\ln\left(\widehat{D}_k\left(IM\right)\right)}{\sqrt{\beta_{D,k}^2+\beta_{C,k|DS_i}^2}}\right] \tag{1}$$

where $\beta_{C,k|DS}$ is the dispersion associated with the capacity. Seismic fragility curves are integrated with the seismic hazard curve in order to evaluate the annual probability of exceeding different levels damage as reported in Eq. (2).

$$PA_{k,i}=\int P\left[DS_{k,i}\left|IM=im\right.\right]\left|\frac{dH\left(im\right)}{dim}\right|dim \tag{2}$$

The annual rate of occurrence of the damage state $i$, for a building component $k$ is approximated by the annual probability of damage due to damage state $i$ only, as in Eq. (3). By assuming a homogeneous Poisson process of seismic events occurrence, the time between damage state occurrences is modeled by the probability density function described by Eq. (4).

$$\lambda_{i,k}=PA_{i,k}-PA_{i+1,k} \tag{3}$$

$$f_{\tau_{i,m}}\left(t\right)=\lambda_{i,m}e^{-\lambda_{i,m}t} \tag{4}$$

This equation reflects the distribution of the time between the beginning of the exposure of the structure to earthquakes ($t=0$) and the occurrence of the first failure ($t=\tau$). Additionally, $C_{k,i}$ is the cost associated with damage state $i$ to restore the building component $k$ to its original configuration. This cost is assumed to remain constant along the service life of the structure, and hence, the expected SLs and its variance can be estimated by using the procedure proposed by Ghosh and Padgett 2011 [10] as follows:

$$E\left[SL_k\right]=\left[\sum_{i=1}^{n}\left(\sum_{t=1}^{T}\lambda_{k,i}e^{-\lambda_{k,i}t}C_{k,i}\right)\right]\cdot\frac{1-\left(1+d\right)^{-T}}{d} \tag{5}$$

$$Var\left[SL_k\right]=\left[\sum_{i=1}^{n}\left(\sum_{t=1}^{T}\lambda_{k,i}e^{-\lambda_{k,i}t}C_{k,i}^2\right)-\left(\sum_{t=1}^{T}\lambda_{k,i}e^{-\lambda_{k,i}t}C_{k,i}\right)^2\right]\cdot\frac{1-\left(1+d\right)^{-2T}}{d\left(2+d\right)} \tag{6}$$

where $T$ represent the remaining service life of the structure and $d$ is the discount rate. The expected value and variance in total seismic loss (TSL) incurred for the whole system and the relative coefficient of variation (CoV) can be determined as:

$$E\left[TSL\right]=\sum_{k=1}^{K}E\left[SL_k\right] \tag{7}$$

$$Var\left[TSL\right]=\sum_{k=1}^{K}Var\left[SL_k\right]+2\sum_{k=1}^{K}\sum_{h=1}^{k-1}\sqrt{Var\left(SL_k\right)Var\left(SL_h\right)}\cdot Corr\left(SL_k,SL_h\right) \tag{8}$$

$$CoV=\frac{\sqrt{Var\left[TSL\right]}}{E\left[TSL\right]} \tag{9}$$

where $Corr\left(SL_k,SL_h\right)$ is the correlation between the SLs for component $k$ and $h$. Cost-benefit analysis is an efficient tool able to provide synthetic information to compare alternative investments and in this case, it is used to compare different retrofit strategies.

## 3 CASE STUDY

A three story ordinary RC moment resisting frame building is considered as case study. The building has been designed for gravity loads only and without any seismic detailing, applying the design rules existing before the introduction of modern seismic codes. The considered frame of the building consists of three stories 3.66 m high and three bays, each 5.49 m wide. Columns have a 300×300 mm$^2$ square section while beams are 230×460 mm$^2$ at each floor. Grade 40 steel ($f_y$ = 276 MPa) and concrete with compression resistance $f_c$' = 24 MPa, were employed in the design. Figure 3-1a shows the general layout of the structure and the position of the braces. The complete detailing may be found in Bracci et al. 1992 [8].

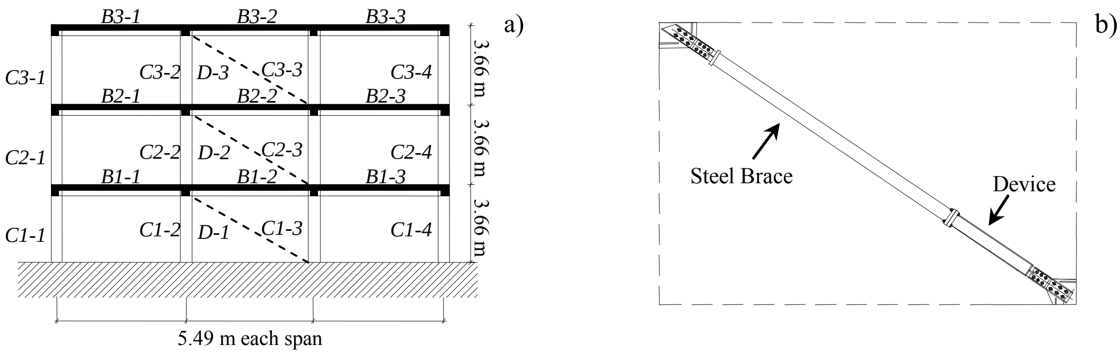


*Figure 3-1 a) General layout of the structure and braces arrangement (adopted from [8]), b) Brace configuration.*

A two-dimensional finite element (FE) model of the structure is developed in OpenSees [11]. The behavior of the BRBs is described by using the Giuffrè-Menegotto-Pinto model with isotropic hardening (Steel02 [11]) while the behavior of SMAs is modeled by using a uniaxial material model based on the phenomenological force-displacement relationship developed by DesRoches et al. 2004 [12]. Extended experimental results are available for a 1:3 reduced scale model of the frame and of its subassemblages. The experimental information include the results of quasi-static lateral load tests of columns and beam-column joint subassemblages, snap back test, white noise excitation test and shaking table tests of the whole frame [8]. The developed FE model is validated by comparing the available experimental results with the simulated test results of the 1:3 scale numerical FE models showing good agreement at global and local scale.

### 3.1 Retrofit cases

The retrofit design method is based on the pushover analysis of the existing frame under a distribution of forces corresponding to its first vibration mode. In this study, the retrofit is performed in order to obtain the same increment of the base shear capacity (40 %) for the same design displacement with all the retrofit techniques. The dissipative braces are made by placing the dissipation device in series with an elastic brace exhibiting adequate over-strength as shown in Figure 3-1b. The stiffness of the dissipative braces is distributed at each story ensures that the first modal shape of the bare frame remains unvaried after the retrofit. This avoids drastic changes to the internal action distribution in the frame, at least in the range of the elastic behavior. In the metallic devices, the strength distribution of the dissipative braces aims at obtaining simultaneous yielding of the devices at all the stories in order to maintain a similar deformation also in the post-elastic range. The brace properties are reported in Table 1. The interested reader is referred to Dall'Asta et al. 2009 [13] for a more detailed description of the design method.

*Table 1 – Brace Properties*

| | BRB | | SMA | |
|---|---|---|---|---|
| $T_1$ | 0.797 sec | | 1.002 sec | |
| Storey | $F^i_d$ [kN] | $K^i_d$ [kN/m] | $F^i_d$ [kN] | $K^i_d$ [kN/m] |
| 1 | 103 | 21565 | 103 | 8513 |
| 2 | 88 | 15020 | 88 | 5929 |
| 3 | 51 | 13713 | 51 | 5413 |

### 3.2 Probabilistic response comparison

In order to describe the probabilistic response of the structures, a set of 240 g.m. records from Baker et al. 2011 [14] have been used to perform NTHAs for the bare frame and the retrofitted frames. The maximum over-time interstory drifts (IDRs) and the story accelerations at each story are used as EDPs in order to evaluate the structural, non-structural and contents damage as suggested in HAZUS-MH 2.0 [7]. The spectral acceleration $S_a(T_1)$ at the fundamental period of the structure $T_1$ for a damping factor $\xi$=5% [15] is employed in this study due to its efficiency. Building location has been considered to be Los Angeles, CA and the seismic hazard curve, $H(a)$ has been obtained from USGS [16] for the Peak Ground Acceleration and successively has been scaled by the spectrum in order to obtain the annual probability of exceeding specified levels of $S_a(T_1)$ for the case study structure. This operation is required for all the different retrofit schemes since the structural period change case by case.

In order to perform the life cycle cost analysis, the remaining service life is assumed as 50 years and the discount rate $d$=0.03. The limit states capacity values and repair cost ratio associated with each limit states are chosen accordingly with HAZUS-MH 2.0 [7] considering that the case study belongs to the building category C1L and building occupancy class COM4 [7]. The Pre-Code seismic design level is considered [7]. Detailed information are reported in Table 2 and Table 3.

*Table 2 – Limit states capacity (according to [7])*

| Components\Limit states | EDPs | Slight | Moderate | Extensive | Complete | $\beta_C$ |
|---|---|---|---|---|---|---|
| Structural | Interstory drift [%] | 0.4 | 0.6 | 1.6 | 4.0 | 0.3 |
| Non-Struct. Drift Sensitive | Interstory drift [%] | 0.4 | 0.8 | 2.5 | 5.0 | 0.3 |
| Non-Struct. Accel. Sensitive | Acceleration [g] | 0.2 | 0.4 | 0.8 | 1.6 | 0.3 |
| Contents | Acceleration [g] | 0.2 | 0.4 | 0.8 | 1.6 | 0.3 |

*Table 3 – Repair Costs (expressed in % of replacement cost according to [7])*

| Components\Limit states | Slight | Moderate | Extensive | Complete |
|---|---|---|---|---|
| Structural | 0.4 | 1.9 | 9.6 | 19.2 |
| Non-Struct. Drift Sensitive | 0.7 | 3.3 | 16.4 | 32.9 |
| Non-Struct. Accel. Sensitive | 0.9 | 4.8 | 14.4 | 47.9 |
| Contents | 1 | 5 | 25 | 50 |

Figure 3-2 reports the PSDMs for the IDR of the 1$^{st}$ story and the story acceleration at the 3$^{rd}$ story of the structure including the results of the bare frame and of the retrofit cases. Figure 3-3 shows the comparison among the fragility curves achieved for the Moderate damage state for structural components at the 1$^{st}$ story and for non-structural acceleration sensitive components at the 3$^{rd}$ story. The comparison among the two retrofit techniques highlight the ability of the diagonal employing BRBs and SMAs in reducing the structural vulnerability (Figure 3-3a), while, as expected from the observation of the PSDMs, all the retrofit systems are similarly inefficient in reducing the non-structural acceleration sensitive components damage (Figure 3-3b).

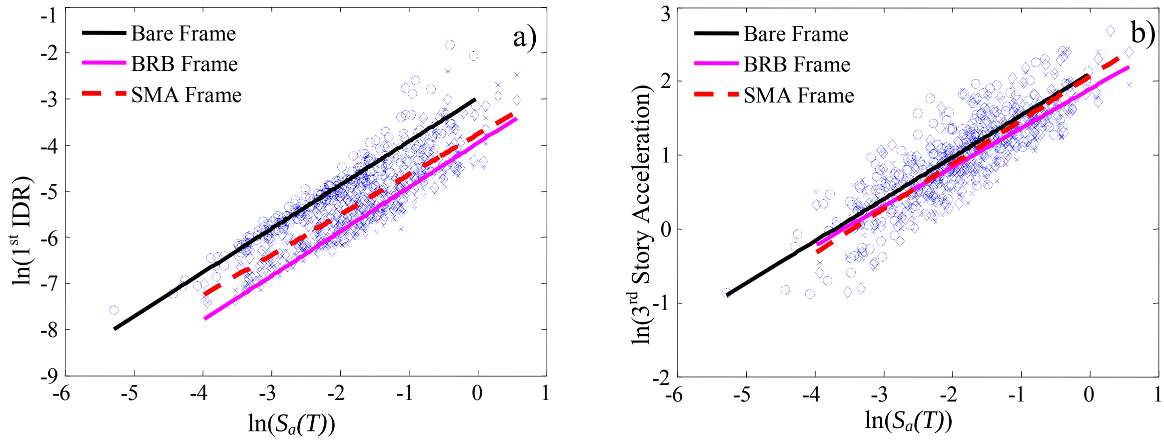


*Figure 3-2 Probabilistic Seismic Demand Model Comparison for: a) Interstory drift at the 1$^{st}$ story b) Story Acceleration at the 3$^{rd}$ story.*

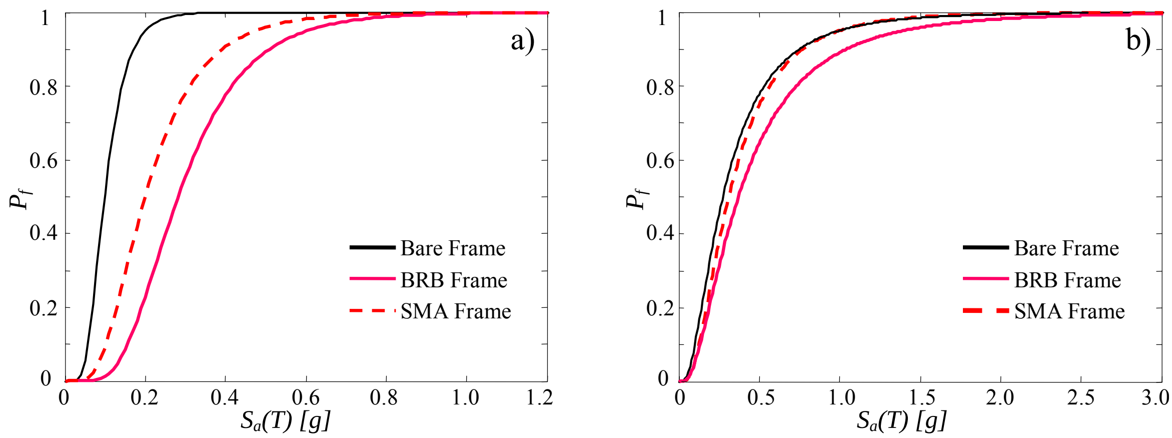


*Figure 3-3 Fragility Curves Comparison at the Moderate Damage Level for: a) Structural Components at the 1$^{st}$ story, b) Non Structural Acceleration Sensitive Components at the 3$^{rd}$ story.*

The convolution of the fragility curves for each component and for each LSs with the hazard curves provides the seismic risk such as reported in Table 4. The table shows the seismic risk connected with the bare frame and with the two retrofitted frames and for all the considered components. As expected from observation of fragility curves, the use of BRBs yields the highest seismic risk reduction in all the components. Finally, the results of the life cycle cost analysis, such as the expected costs and its CoV are reported in Table 5. It is observed that the use of BRBs yields to the highest loss saving and at the same time the lower CoV with respect to the SMAs.

*Table 4 – Seismic Risk*

| | | Components\Limit states | Slight | Moderate | Extensive | Complete |
|---|---|---|---|---|---|---|
| Bare Frame | Story 1 | Structural | 4.25E-02 | 2.30E-02 | 3.32E-03 | 2.60E-04 |
| | | Non-Struct. Drift Sensitive | 4.25E-02 | 1.41E-02 | 1.06E-03 | 1.23E-04 |
| | | Non-Struct. Accel. Sensitive\Contents | 4.49E-02 | 7.69E-03 | 7.02E-04 | 3.08E-05 |
| | Story 2 | Structural | 5.62E-02 | 3.14E-02 | 4.92E-03 | 4.09E-04 |
| | | Non-Struct. Drift Sensitive | 5.62E-02 | 1.97E-02 | 1.62E-03 | 1.95E-04 |
| | | Non-Struct. Accel. Sensitive\Contents | 5.08E-02 | 9.00E-03 | 8.18E-04 | 3.33E-05 |
| | Story 3 | Structural | 4.96E-02 | 2.20E-02 | 1.45E-03 | 3.13E-05 |
| | | Non-Struct. Drift Sensitive | 4.96E-02 | 1.13E-02 | 2.67E-04 | 9.71E-06 |
| | | Non-Struct. Accel. Sensitive\Contents | 4.09E-02 | 6.73E-03 | 5.25E-04 | 1.65E-05 |
| BRB Frame | Story 1 | Structural | 1.24E-02 | 5.19E-03 | 3.58E-04 | 1.21E-05 |
| | | Non-Struct. Drift Sensitive | 1.24E-02 | 2.58E-03 | 7.82E-05 | 4.47E-06 |
| | | Non-Struct. Accel. Sensitive\Contents | 3.94E-02 | 5.38E-03 | 3.80E-04 | 1.27E-05 |
| | Story 2 | Structural | 1.71E-02 | 7.36E-03 | 5.19E-04 | 1.69E-05 |
| | | Non-Struct. Drift Sensitive | 1.71E-02 | 3.70E-03 | 1.13E-04 | 5.99E-06 |
| | | Non-Struct. Accel. Sensitive\Contents | 4.56E-02 | 6.32E-03 | 4.07E-04 | 1.07E-05 |
| | Story 3 | Structural | 1.19E-02 | 4.12E-03 | 1.38E-04 | 1.46E-06 |
| | | Non-Struct. Drift Sensitive | 1.19E-02 | 1.72E-03 | 1.85E-05 | 3.64E-07 |
| | | Non-Struct. Accel. Sensitive\Contents | 5.11E-02 | 6.45E-03 | 3.37E-04 | 6.09E-06 |
| SMA Frame | Story 1 | Structural | 2.02E-02 | 8.96E-03 | 6.95E-04 | 2.59E-05 |
| | | Non-Struct. Drift Sensitive | 2.02E-02 | 4.64E-03 | 1.58E-04 | 9.83E-06 |
| | | Non-Struct. Accel. Sensitive\Contents | 2.88E-02 | 4.36E-03 | 3.54E-04 | 1.39E-05 |
| | Story 2 | Structural | 2.64E-02 | 1.27E-02 | 1.32E-03 | 7.07E-05 |
| | | Non-Struct. Drift Sensitive | 2.64E-02 | 7.08E-03 | 3.54E-04 | 3.01E-05 |
| | | Non-Struct. Accel. Sensitive\Contents | 3.37E-02 | 5.19E-03 | 3.91E-04 | 1.26E-05 |
| | Story 3 | Structural | 1.93E-02 | 8.31E-03 | 5.91E-04 | 1.89E-05 |
| | | Non-Struct. Drift Sensitive | 1.93E-02 | 4.21E-03 | 1.26E-04 | 6.82E-06 |
| | | Non-Struct. Accel. Sensitive\Contents | 3.56E-02 | 5.37E-03 | 3.77E-04 | 1.05E-05 |

*Table 5 – Life cycle cost Analysis results*

| | Expected Cost (LCC) [% of Replacement Cost] | CoV | Loss Saving |
|---|---|---|---|
| Bare Frame | 309.69 | 0.0616 | - |
| BRB Frame | 160.98 | 0.0717 | 148.71 |
| SMA Frame | 174.50 | 0.0723 | 135.19 |

## 4 CONCLUSION

A complete methodology allowing the comparison of different retrofit techniques of seismic passive control of buildings is proposed and applied in this paper. A three story ordinary moment resisting RC frame is used as case study and the effectiveness of two different devices is investigated. The effectiveness of each retrofit method is evaluated in terms of seismic risk reduction and by performing a life cycle cost analysis and defining the loss saving for each retrofit case. By using this comprehensive parameter the results show that the dissipative braces employing BRBs are more cost effective. Future developments of the present work are focused on highlighting the capability of SMAs in residual drift reduction by accounting of appropriate EDPs. Moreover, the use of local EDPs may be useful in order to have a deeper description of the advantages obtained by the retrofit techniques and a more accurate evaluation of the expected seismic losses.

## REFERENCES


[1] Soong, T.T. & Spencer, B.F. 2002. Supplemental energy dissipation: state-of-the-art and state-of-the-practice. *Engineering Structures*, 24(3) 243-259.

[2] Chang, S.E. & Shinozuka, M. 1996. Life-cycle cost analysis with natural hazard risk. *Journal of Infrastructure System*, 2(3) 118-126.

[3] Wen, Y.K. 2001. Reliability and performance-based design, *Structural Safety*, 23(4) 407-428.

[4] Wen, Y.K. & Shinozuka, M. 2001. Cost-effectiveness in active structural control. *Engineering Structures*, 20(3) 216-221.

[5] Wen, Y.K. & Kang, Y.J. 2001. Minimum building life-cycle cost design criteria. I: methodology, *Journal of Structural Engineering*, 127(3) 330-337.

[6] Padgett, J.E., Dennemann, K. & Ghosh, J. 2010. Risk-based seismic life-cycle cost-benefit (LCC-B) analysis for bridge retrofit assessment. *Structural Safety*, 32 165-173.

[7] FEMA. 2003. Earthquake model. HAZUS-MH 2.0: Technical Manual. Federal Emergency Management Agency, Washington DC.

[8] Bracci, J.M., Reinhorn, A.M. & Mander, J.B. 1995. Seismic resistance of reinforced concrete frame structures designed for gravity loads: performance of structural system. *ACI Structural Journal*, 92(5) 597-608.

[9] Cornell, C. A., Jalayer, F., Hamburger, R.O. & Foutch, D.A. 2002. Probabilistic Basis for 2000 SAC Federal Emergency Management Agency Steel Moment Frame Guidelines, *Journal of Structural Engineering*, 128(4) 526-533.

[10] Ghosh, J. & Padgett, J. E. 2011. Probabilistic seismic loss assessment of aging bridges using a component-level cost estimation approach. *Earthquake Engineering & Structural Dynamics*, 40(15) 1743-1761.

[11] McKenna, F., Fenves, G.L. & Scott, M.H. 2006. OpenSees: Open system for earthquake engineering simulation. Pacific Earthquake Engineering Center, University of California, Berkeley, CA.

[12] DesRoches, R., McCormick, J. & Delemont, M. 2004. Cyclic properties of superelastic shape memory alloy wires and bars, *Journal of Structural Engineering*, 130(1) 38–46.

[13] Dall'Asta, A., Ragni, L., Tubaldi, E. & Freddi, F. 2009. Design methods for existing r.c. frames equipped with elasto-plastic or viscoelastic dissipative braces. *Proceedings of XIII Convegno Nazionale ANIDIS*, Bologna, Italy.

[14] Baker, J., Jayaram, B. & Shahi, S. 2011. Ground Motion Studies for Transportation Systems. *PEER Website*, (http://peer.berkeley.edu/transportation/projects/ground-motion-studies-for-transportation-systems/).

[15] Katsanos, E.I., Sextos, A.G. & Manolis, G.D. 2009. Selection of earthquake ground motion records: A state-of-the-art review from a structural engineer prospective. *Soil Dynamics and Earthquake Engineering*, 30(4) 157-169.

[16] USGS, United States Geological Survey. (http:// www.usgs.gov/).